High resolution-ion mobility mass spectrometry as an additional powerful tool for structural characterization of mycotoxin metabolites

High resolution-ion mobility mass spectrometry as an additional powerful tool for structural characterization of mycotoxin metabolites.

Laura Righetti[1,2], Marie Fenclova[1], Luca Dellafiora[2], Jana Hajslova[1], Milena Stranska-Zachariasova[1*], Chiara Dall'Asta [2].

[1] Department of Food Analysis and Nutrition, Faculty of Food and Biochemical Technology, University of Chemistry and Technology, Prague, Technicka 3, 166 28 Prague 6, Czech Republic

[2] Department of Food and Drug, University of Parma, Parco Area delle Scienze 17/A, 43124 Parma, Italy

Corresponding authors details:
Prof. Milena Stranska-Zachariasova, Ph.D.
Department of Food Analysis and Nutrition, University of Chemical Technology, ~~Technická~~ Technicka 3, Prague 6, CZ-166 28, Czech Republic.
E-mail: milena.stranska@vscht.cz

Abstract

This work was designed as a proof of concept, to demonstrate the successful use of the comparison between theoretical and experimental collision cross section (CCS) values to support the identification of isomeric forms. To this purpose, thirteen mycotoxins were considered and analyzed using drift time ion mobility mass spectrometry. A good linear correlation (R^2 - r^2 = 0.962) between theoretical and experimental CCS was found. The average ΔCCS was 3.2%, fully consistent with the acceptability threshold value commonly set at 5%. The agreement between theoretical and experimental CCS obtained for mycotoxin glucuronides suggested the potential of the CCS matching in supporting the annotation procedure.

Keywords: Modified mycotoxins; drift-time ion mobility mass spectrometry; metabolite structural characterization.~~; High resolution mass spectrometry.~~

Chemical compounds studied in this article: Alternariol (PubChem CID: 5359485); alternariol monomethyl ether (PubChem CID: 5360741); deoxynivalenol (PubChem CID: 40024); zearalenone (PubChem CID: 5281576); deoxynivalenol 3-glucuronide (PubChem CID: 102202100); deoxynivalenol 15-glucuronide (PubChem CID: 102202102); zearalenone 14-glucuronide (PubChem CID: 71753018).

Formatted: Font: Italic

1. Introduction

Mycotoxins are toxic secondary metabolites produced by a large number of fungal species, potentially infesting foodstuffs at all stages of food production, processing and storage. Therefore, humans and animals can be simultaneously exposed through the diet to "cocktails" of mycotoxins (Hove, Van Poucke, Njumbe-Ediage, Nyanga & De Saeger, 2016; Smith, Madec, Coton & Hymery, 2016; Assunção, Silva & Alvito, 2016). However, the possible extent and the combined effects of co-exposure in humans and animals~~,~~ are still to be defined (Alassane-Kpembi, Puel, Pinton, Cossalter, Chou & Oswald, 2017; Shirima, 2015). Current risk assessment involves the estimation of the exposure, based on the combination of estimation food consumption data with co-occurrence data collected by control agencies (Heyndrickx, 2014). Although very useful for risk management, this approach is based on a severe approximation, as average co-occurrence data obtained for each food category~~,~~ are projected on food consumption data averaged throughout the EU population. Therefore, this under/over-estimation may affect the regulatory action, leading to less effective policies.

In the era of personalized healthcare, a more individual-focused exposure assessment could be obtained by measuring the levels of relevant biomarkers in urine (Ali, Muñoz & Degen, 2017; Föllmann, Ali, Blaszkewicz & Degen, 2016; Wallin, 2015; Heyndrickx, Sioen, Huybrechts, Callebaut, De Henauw & De Saeger, 2015). ~~However, the identification of proper biomarkers for mycotoxins implies the full elucidation of their toxicokinetics, also in view of the inter-individual variability due to epigenetic-related phenomena (Mukherjee, 2014; Warth, Sulyok, Berthiller, Schuhmacher & Krska, 2013).~~

Glucuronidation is one of the main phase II metabolic pathways, whereby mycotoxins, ~~such~~ in a similar way to~~as~~ other natural compounds occurring in the diet and drugs, are biotransformed into polar conjugates, before excretion in bile or urine (Warth, 2013). The reaction is mediated by a family of membrane-bound

enzymes, UDP-glucuronosyltransferases (UGTs), ~~that~~ whch catalyze the transfer of glucuronic acid to a nucleophilic functional group of the target compound. In humans, up to 20 different UGT isoforms have been characterized, following expression of their corresponding cDNA in heterologous cells (Ritter, 2000). Studies have shown that these isoforms present distinct, but frequently overlapping, substrate specificities, leading therefore to the formation and excretion of a range of isomeric glucuronides of the same xenobiotic (Tripathi, Bhadauriya, Patil & Sangamwar, 2013; Dong, Ako, Hu, & Wu, 2012; Wu, Basu, Meng, Wang & Hu, 2011).

Besides their urinary excretion as biomarkers, regio- and stereospecificity in isomers formation are relevant also in consideration of the possible differences in their biological activity. Although glucuronidation is indeed often regarded as a detoxification process, in some cases the xenobiotic glucuronidation may elicit biologically active or toxic metabolites, i.e. morphine-6-glucuronide is a more potent opioid agonist than morphine itself (Ritter, 2000). Similarly, DON-15-glucuronide has been predicted, according to computational calculation, to be more ribotoxic than its parent compound (Dellafiora, Galaverna & Dall'Asta, 2017).

Concerning mycotoxins, the glucuronidation pathways of deoxynivalenol (DON), zearalenone (ZEN), ochratoxin A (OTA), alternariol (AOH) and its methyl ether (AME), have been partially or fully elucidated so far, also in terms of the activity of different human UGT isoforms (Maul, Warth, Schebb, Krska, Koch & Sulyok, 2015; Maul, 2012; Pfeiffer, Schmit, Burkhardt, Altemöller, Podlech & Metzler, 2009; Pfeiffer, Hildebrand, Mikula & Metzler, 2010).

Besides inter-species variability (Maul, 2012, Welsch & Humpf, 2012; Maul, 2015), inherent factors, such as gender, age and epigenetics, may affect the glucuronidation, and therefore have an impact on the pattern of urinary biomarkers (Videmann, Koraichi, Mazallon & Lecoeur, 2012; Yasar, Greenblatt, Guillemette & Court, 2013; Dluzen, 2014).

Glucuronidation studies are often performed using liver microsomes or microsomal fractions from different animals, to explore possible inter-species differences leading to a different biomarker pattern in urine and/or plasma (Welsch, 2012). Specific enzymes can be isolated, as well.

Once different glucuronides are obtained upon incubation, further steps of isolation and purification are required before structural elucidation, which is usually performed by NMR analysis. However, although efficient for evaluating isomeric heterogeneity, the main limitation of this approach is the need ~~of~~ for a considerable amount of pure analyte.

In this frame, a new analytical technique, ion mobility spectrometry (IMS), is gaining wider recognition as a promising approach that can overcome the above-mentioned NMR limitations, making it an ideal candidate for improving confidence in the identification and separation of structurally closely related isomers (Righetti, Paglia, Galaverna & Dall'Asta, 2016). IMS is a gas-phase electrophoretic technique that provides a new dimension (3D) of separation based on size, shape, and charge of ions (Cumeras, Figueras, Davis, Baumbach & Gràcia, 2015; Paglia et al. 2015a; Paglia, Kliman, Claude, Geromanos & Astarita, 2015b). So far, three major IMS-MS separation approaches are currently commercially available: drift-time IMS (DT-IMS), traveling-wave IMS (TW-IMS), and high field asymmetric waveform IMS (FAIMS), also known as differential-mobility spectrometry (DMS) (Cumeras, 2015; Paglia, 2015a; Paglia, 2015b). In DT-IMS (May, 2014), ions move through a homogeneous, continuous electric field in a drift tube in the presence of neutral gas molecules. DT-IMS consists of a series of stacked-ring electrodes where a near-uniform electric field is created along the axis of the drift tube. The carrier gas and the gaseous sample are introduced into the ionization region, while a counter current flow of a neutral gas (mostly nitrogen, helium or argon), is introduced from the side of the detection region (Cumeras, 2015). Thus, species with the same mass-to-charge ratio (i.e., isomers) can be separated according to their ability to pass through a tube filled with a gas under the influence of an electric field.

Since isomers, such as those obtained upon glucuronidation, have the same mass-to-charge ratio, but a different three-dimensional (3D) conformation, the time taken for each parent ion to drift through the tube will be significantly different. Since the ion drift time depends principally on the collision frequency between the ions and the buffer gas (Paglia, 2015a), it allows the measurement of the collision cross section (CCS) values, according to the Mason-Schamp equation (May, 2014).

On the other side, being related to the unique structural conformation of the molecule, the CCS value can be calculated by theoretical computation (Lapthorn, Pullen, Chowdhry, Wright, Perkins & Heredia, 2015; Boschmans, 2016), offering therefore a powerful tool for structural imputation in the absence of reference compounds.

To prove the effectiveness of IMS-MS in supporting the structural identification of isomeric glucuronides through the comparison of theoretical and experimental CCS values, this study was aimed at the HR-MS characterization of the glucuronides obtained by incubation of four possible co-occurring mycotoxins, i.e. DON, ZEN, AME, and AOH, with human liver microsomes.

Materials and Methods

Chemicals and reagents

Mycotoxin standards of AOH, AME and ZEN were purchased from Sigma (Stuttgart, Germany). Analytical standard of DON was purchased from Romer Labs® (Tulln, Austria). ~~HPLC~~ HPLC-grade~~-~~ solvents methanol, acetonitrile and acetic acid were obtained from Sigma (Stuttgart, Germany). Double ~~Bi~~distilled water was obtained by a Milli-Q purification system (Millipore, Bedford, MA~~, USA~~). Human liver microsomes were purchased from Sigma Aldrich and stored at ~~-~~ ~~-~~80 °C. Uridine 5′-diphosphoglucuronic acid (UDPGA), uridine 5′-diphospho-*N*-acetylglucosamine (UDPGN), Tris-HCl and $MgCl_2$ were purchased from Sigma-Aldrich (St. Louis, MO).

Formatted: Font: Italic

Glucuronidation assay

Human liver microsomes were individually incubated with AOH, AME, ZEN and DON, following the protocols already reported in the literature (Pfeiffer, 2009; Pfeiffer, 2010; Maul, 2012; Uhlig, 2013). Briefly, the incubation mixture contained 3.75 mM of each mycotoxin~~s~~, 7.4 mM UDPGA, 50 mM Tris-HCl buffer (pH 7.4), 8 mM $MgCl_2$, 0.3 mM UDPGN, and 100 µL of liver microsomes in a total volume of 0.5 mL. The incubation was performed at 37 °C for 60 min in a shaking water bath and stopped by adding acetonitrile (1:1; *v/v*). Protein ~~were~~ was precipitated after centrifugation

Formatted: Font: Italic

(4000 *g* for 5 min) and the supernatant was evaporated to dryness and reconstructed in methanol. Glucuronides were purified from the unreacted parent mycotoxins by means of semi-preparative HPLC (1525 Binary HPLC~~,~~ ~~;~~ Waters) equipped with UV detector (998; Waters) using a Synergi fusion C18 column (80Å, 150 ×~~x~~ 10 mm) and ~~bidistilled~~ double-distilled water~~s~~ and methanol (both acidified ~~(~~with 0.2% formic acid) as mobile phases.

Measurements of the exact mass and the fragmentation patterns of glucuronide isomers were performed by UHPLC-IM-QTOFMS.

UHPLC-IM-QTOF analysis

~~UHPLC~~ Agilent 1290 Infinity ~~LC~~ UHPLC system coupled to commercial prototype IM-MS, which incorporates a drift tube coupled to a quadrupole time-of-flight mass spectrometer (IM-Q-TOFMS, Agilent Technologies, Santa Clara, CA) was employed. An orthogonal electrospray ionization (ESI) source (Agilent Jet Stream) was used.

For the chromatographic separation of ZEN, AOH and AME glucuronides, a reversed-phase C18 Acquity HSS T3 column (2.1 × 100 mm and a particle size of 1.8 µm; Waters) ~~with 2.10×100 mm and a particle size of 1.8 µm~~ heated to 40 °C was used. Gradient elution was performed by using ~~bidistilled~~ double-distilled water (eluent **A**) and acetonitrile (eluent **B**), both acidified with 0.5% acetic acid. From the initial conditions set at 20% **B**, eluent **B** was increased to 40% in 5 min and to 95% in 1 min~~.~~ ~~;~~ ~~after~~ After an isocratic step (2 min), the system was re-equilibrated to initial conditions for 2 min. The total run time was 10 min and flow rate was set at 0.300 ~~ml~~mL/min.

By contrast, for the separation of DON-GlcAs an Acquity UPLC BEH Amide column (1.7 µm; 2.1 mm ×~~x~~ 100 mm) was used; gradient elution was performed as previously described (Zachariasova, Vaclavikova, Lacina, Vaclavik, & Hajslova, 2012).

The autosampler temperature was kept at 5 °C; 10 µL of sample ~~was~~ were injected into the system. The ESI source was operated in negative ionization mode (ESI^-) with a nitrogen sheet gas temperature at 400 °C at a flow rate of 12 L/min and the following voltages: capillary 4500 V,

Formatted: Font: Italic

Formatted: Font: Bold

Formatted: Font: Bold

Formatted: Font: Bold

Formatted: Font: Bold

nozzle 1700 V. Nitrogen drying gas applied at the source entrance was heated at 150 °C at a flow rate of 10 mL/min. The ion mobility drift gas pressure (nitrogen) was maintained at 4 Torr and 28.8 °C; the drift tube entrance voltages were set to 1700 V.

The QTOF spectrometer operated in full scan mode from *m/z* 50 to 1000 ~~m/z~~ and ions were targeted for ~~collision~~ collision-induced dissociation (CID) fragmentation based on the previously determined accurate mass and retention time.

Formatted: Font: Italic

Calculation of experimental Collision Cross Section values

Drift tube ion mobility provides a direct accurate method to calculate the CCS (Ω) using the Mason-Schamp equation (Mason & Schamp, 1985). Considering that the Mason~~-~~-Schamp equation defines CCS as a function of several experimental parameters, these parameters must be well-characterized to obtain CCS values with high confidence. In particular, drift tube length, temperature, pressure and drift voltage should be carefully checked before each CCS measurement. The~~r~~se parameters indeed, are the major factors that contributed to total uncertainty of drift time measurement.

IM-MS Browser (Agilent Technologies) was employed for data acquisition and processing. First, the drift ramp method with ~~infusion~~ infusion-based acquisition was applied with calibration solution. The method consists of time segments in a single acquisition, each segment with a different drift tube voltage (1000 – 1700 V with ~~100~~ 100-V steps). The calibration factor was calculated based on the known calibrant CCS values and this factor was applied to the next sample ~~analyzes~~analyses. ~~10 µL~~Ten microlitres of sample ~~was~~ were injected onto the column and measured without any changes of source conditions and within the ion optics following the drift tube. Instead of the ~~time~~ time-segmented acquisition, the analysis was sequentially repeated with ~~the~~ different drift tube voltages (1100, 1300, 1500 and 1700 V). Using the calibration factor and reference CCS (243 $Å^2$) from the reference mass 922, the CCS values for the ions of interest were calculated. On

the basis of a propagation-of-error analysis, including the limits of precision for experimental parameters, the accuracy of all CCS values was estimated to be better than 2% (May, 2014).

Calculation of theoretical collision cross section values

The calculation of the theoretical CCS values relied on the three-dimensional (3D) atomic coordinates of the molecules under investigation. In particular, ~~A~~all the 3D structures of aglycones are freely available and they were retrieved from the PubChem database (Kim, 2016). Conversely, ~~,~~ ~~while all~~ none of the glucuronide derivatives has been made available so far. Therefore, all of them were obtained computationally, ~~processed~~editing ~~from~~ the respective aglycones ~~by~~ with the addition of glucuronic acid groups, using ~~using~~ the software Sybyl, version 8.1 (www.certara.com), as previously reported (Cozzini & Dellafiora, 2012). For each 3D structure, ~~A~~all the atoms were checked for the atom- and bond-type assignments, correcting any erroneous attributions. Then, atom~~s~~ c~~C~~harges ~~were~~ were calculated and assigned using the MMFF94 method ~~in Sybyl. and each~~ Afterwards, all the 3D structures were~~molecule was~~ energetically minimized using the Powell algorithm ~~whit~~ with a coverage gradient of ≤ 0.05 kcal (mol Å)~~-~~$^{-1}$ and a maximum of 500 cycles. In order to calculate the theoretical CCS values, such optimized 3D structure~~s~~ were used as input in a modified version of the Mobcal software that simulates the condition of nitrogen buffer gas instead of helium (Campuzano, Bush, Robinson, Beaumont, Richardson & Kim, 2012; Kim, Kim, Johnson, Beegle, Beauchamp & Kanik, 2008; Mesleh, Hunter, Shvartsburg, Schatz & Jarrold, 1996). In particular, the default setting has been used with a temperature of 300 K. As an exception, in order to speed up computing time, the number of points in the Monte Carlo integrations of MOBIL2 impact parameter and orientation was set at 50, while the number of points in MOBIL2 velocity integration was set at 40.

All the volume and area values were calculated by using UCSF Chimera software, version 1.1 (Pettersen, 2004)

Field Code Changed

The correlation between tCCS and eCCS values were evaluated using the Kendall Tau test with ~~Statistical analysis was performed using~~ IBM SPSS Statistics v.23 (SPSS Italia, Bologna, Italy).

Results and Discussion

Glucuronidation of target mycotoxins

This work was designed as a proof of concept, to demonstrate the successful use of the comparison between theoretical and experimental CCS values, to support the identification of isomeric forms. Therefore, target mycotoxins were selected according to two conditions: a) the presence of at least two sites for glucuronidation; b) availability in the literature of information about the formation of isomeric glucuronides. Accordingly, DON, ZEN, AME and AOH were selected, as fully matching the requirements (Figure 1).

DON is the main *Fusarium* mycotoxin occurring in cereals and products thereof worldwide. After oral absorption, it undergoes glucuronidation in the liver, giving rise to both DON-3GlcA and DON-15GlcA isomers. A third minor isomer, putatively annotated as DON-7GlcA, has been reported by some authors, but not yet structurally elucidated (Maul, 2012; Uhlig, Ivanova & Fæste, 2013). According to the literature (Warth, 2012; Warth, Sulyok & Krska, 2013; Heyndrickx, 2015), the ratio DON-15GlcA/DON-3GlcA in humans is approximately 3~~/~~:1.

ZEN is an estrogenic mycotoxin, undergoing extensive phase I and phase II metabolism in living organisms. According to recent studies, besides the glucuronidation of phase I metabolites, it is directly metabolized into ZEN-14GlcA, which is ~~largely~~ the main glucuronide formed by human liver microsomes, in consideration of the steric~~al~~ hindrance due to the strong hydrogen bonding between the hydroxyl group at C16 and carbonyl group at C1 (Pfeiffer, Hildebrand, Mikula & Metzler, 2010).

Formatted: Font: Italic

Concerning *Alternaria* mycotoxins, glucuronidation of AOH and AME mainly occurs at position 3, giving rise to AOH-3GlcA and AME-3GlcA. In addition, AOH-9GlcA is also formed, while glucuronidation at position 7 seemed to be strongly hindered (Pfeiffer, 2009).

To obtain glucuronide mixtures for further analysis, the target mycotoxins were incubated with human hepatic microsomes in the presence of UDPGA (7.4 mM in 500 µL). The pool was then ~~analysed~~ analyzed by UHPLC-Q-TOF for identification. Data are reported in Table 1.

In our mixture, only one ZEN conjugate was detected (Figure 1, ~~*supplementary*~~ *Supplementary* ~~*material*~~*Material*). It had a quasimolecular ion of *m/z* 493.1720, which gave rise to fragment ions of 317.1395, corresponding to the loss of glucuronic acid (176.0315 amu) and *m/z* 175.0245 resulting from the loss of the aglycone from the quasimolecular ion (Table 1). Therefore, in agreement with the literature, this metabolite was annotated as ZEN-14GlcA, since the isomer ZEN-16GlcA differs in the fragmentation pathway, involving also the loss of carbon dioxide (44.0095 amu) [6].

Incubation of DON with human liver microsomes gave rise to two isomeric glucuronides, in agreement with previous literature (Uhlig, 2013). The two glucuronidation products afforded primarily ions with *m/z* 471.1508 in negative ionization mode (Figure ~~2~~ 2, ~~*supplementary*~~ *Supplementary* ~~*material*~~*Material*). However, their MS/MS spectra differ ~~for~~ due to the presence of *m/z* 441.1422 fragment that is likely to arise from cleavage of the CH_2OH moiety attached al C-6 (Dall'Asta, Berthiller, Schuhmacher, Adam, Lemmens & Krska, 2005). This loss is consistent with the fragmentation pattern of the minor isomer DON-3GlcA.

When AME was incubated with human liver microsomes, two glucuronides with quasimolecular negative ions at *m/z* 447.0950 and fragment ions at *m/z* 271.0609 and 175.0237 were obtained. The two HRMS/MS spectra were very similar (Figure 3, ~~*supplementary*~~ *Supplementary* ~~*material*~~*Material*~~),~~); thus the assignment of the glucuronic acid moiety was not possible. However, considering that AME has only two hydroxyl groups, the major glucuronide is proposed to be AME-3GlcA and the minor glucuronide AME-7GlcA, in agreement with previous

Formatted: Font: Not Italic

Formatted: Font: Not Italic

Formatted: Font: Italic

Comment [JS1]: Wrong reference style

Formatted: Font: Not Italic

Formatted: Font: Italic

Formatted: Font: Not Italic

findings (Pfeiffer, 2009). However, based on HR-MS analysis, the univocal identification of the isomers was not possible.

Regarding AOH glucuronidation, three glucuronide conjugates were detected in our study (see Figure 2), in contrast with the literature reporting only the formation of AOH-9GlcA and AOH-3GlcA (Pfeiffer, 2009). HRMS/MS spectra of the three glucuronides were almost identical, with a molecular ion of *m/z* 433.0779 and fragment ions corresponding to the loss of glucuronic acid (*m/z* 257.0456) and ~~to~~ the loss of the aglycone (*m/z* 175.0245). In consideration of the steric~~al~~ hindrance of the hydroxyl group in position 7 compared to position 9 and 3, the most abundant peaks were tentatively attributed to AOH-3GlcA and AOH-9GlcA, while the third detected glucuronide (about 0.7% of the total glucuronidated forms) was tentatively annotated as AOH-7GlcA. As for AME glucuronides, based on HRMS analysis, the univocal identification of the isomers was not possible.

Calculation of the experimental CCS vs th~~ree~~eoretical CCS values

To explore the possible application of ion mobility spectrometry to support structural identification of the isomeric glucuronides of selected mycotoxins, their experimental CCS (eCCS) values were measured in the drift tube. For the same set of compounds, the theoretical CCS (tCCS) values were calculated using $N_{2(g)}$ parameterized MOBCAL software. Experimental and theoretical CCS values, along with structural parameters, are reported in Table 2.

As expected, the eCCS values were found to be significantly correlated with their respective volume (Kendall Tau correlation, $\tau = 0.646$, $p = 0.003$). A good correlation was found for eCCS values and molecular mass as well (Kendall Tau correlation, $\tau = 0.576$, $p = 0.009$). Since the mobility of molecules strongly depends on their collision with the drift gas, molecular mass and volume are good descriptors of the phenomena (Paglia, 2015a; Paglia, 2015b; Goscinny, Joly, De Pauw, Hanot & Eppe, 2016). However, CCS values are mostly related ~~on~~ to the spatial arrangement of each compound, which may differ significantly between isomeric forms (see Figure 3).

Formatted: Font: Not Italic

Formatted: Font: Italic

Formatted: Font: Italic

Formatted: Font: Italic

Formatted: Font: Italic

Formatted: Font: Not Italic

The main advantage of the use of CCS values for compound identification is ~~due to~~ their independence from both the concentration of the target compound and the sample matrix (Goscinny, 2016). ~~Taking into account the analytical efforts made in the last years for validating extraction and detection procedure depending on the sample matrix, the great advantage offered by the CCS values as molecular descriptor is evident, especially when metabolites occurring at low traces in biological fluids are considered.~~

However, the experimental evaluation of CCS values, as well as their matching with theoretical values, still presents some limitations, mainly due to the instrumental set up used for drift time measurement. To overcome this problem, proper correction models should be implemented, aimed at comparing the eCCS with tCCS. However, the implementation of such models requires the availability of large datasets of compounds, with a great chemical diversity, evenly distributed over a wide range of masses and volumes. In addition, the possible formation of protomers and adducts may significantly affect the measurement of eCCS, and therefore must be carefully considered in the development of the model.

In our set, it must be considered that the masses of the target analytes ranged between *m/z* 257 and 493 ~~m/z~~; all the compounds have been measured as [M – H]$^-$ ions, although all of them presented several deprotonation sites. These are important parameters for setting the eCCS *vs* tCCS comparison, as reported by different authors (Lapthorn, 2015; Boschmans, 2016). Among possible factors, the protonation/deprotonation site can affect significantly the drift times. This effect can actually be relatively large for small molecules (Boschmans, 2016).

On plotting the tCCS values for the lowest energy structure *vs* eCCS, a good linear correlation between the eCCS and tCCS was observed, with an R^2-r^2 value of 0.962 (Figure 4). This indicates that the model is able to measure CCS values of other molecules whit acceptable reliability. The percentage of error calculated as the deviation between eCCS and tCCS ranged from 0.7 to 8.8%, as reported in Table 2. This is in line with the finding of Gonzales et al. (Gonzales, Smagghe, Coelus,

Formatted: Font: Italic

Formatted: Font: Italic

Formatted: Font: Italic

Formatted: Font: Not Italic

Formatted: Font: Not Italic

Adriaenssens, De Winter & Van Camp, 2016) that reported a percentage of error ranging from 0.6 to 9.6% when comparing eCCS and tCCS for 56 deprotonated phenolics. The average ΔCCS was 2.3%, therefore fully consistent with the acceptability threshold value commonly set at 5% (Paglia, 2015a). Among the calculated set, only DON showed a ΔCCS > 5% (i.e. 8.8%). Since experimental data have been collected for [M – H]- species, and DON is the only compound in the set with slightly deprotonable groups (i.e alcoholic hydroxyl groups *vs* phenolic or carboxylic hydroxyl groups), this might affect the agreement between eCCS and tCCS.

In the case of DON glucuronides, CCS values could not support confirmation of the annotation, as eCCS were 199.0 Å and 200.7 Å for DON-3GlcA and DON-15GlcA, respectively. In consideration of a mean experimental error of 2% obtained by DT-IM, these values do not significantly differ under the experimental conditions applied. This is however in agreement with the very similar eCCS values obtained (see Table 2).

Considering AME and its glucuronides, although tCCS values are always lower than the respective eCCS values, the rank is consistent (AME < AME-3GlcA < AME-7GlcA). Therefore, this data, along with the fragmentation pattern, may be used as a confirmation for the given annotation.

The agreement between tCCS and eCCS for AOH and its glucuronides is lower than those obtained for other mycotoxins. However, the relative rank of compounds (AOH < AOH-9GlcA < AOH-3GlcA < AOH-7GlcA) supported the given annotation.

In consideration of the small set of compounds considered within this study and the aforementioned limitations, the good fitting obtained is very promising. In particular, the rank between each parent compound and its glucuronides is always consistent, and this supports the possible inclusion of CCS values in the annotation procedure.

Formatted: Font: Italic

Formatted: Font: Not Italic

Formatted: Indent: First line: 1.25 cm, Don't allow hanging punctuation, Font Alignment: Baseline

An enlargement of the set, with the inclusion of different classes of compounds distributed along a larger range of molecular masses, together with a step-by-step refining of the experimental parameters, may support a fine tuning of the computational model.

On the other side, studies have to be undertaken to evaluate the stability of eCCS in different matrices and under different experimental/instrumental conditions. In particular, due to the fact that different IMS strategies are available on the market, a comparison of CCS values obtained on different instruments and with different instrumental set-up, has to be considered as a future step.

Similarly, tools for tCCS calculations should be implemented and fine-tuned to obtain reliable data, especially for multi-charged ions and adducts.

~~In particular, the rank between each parent compound and its glucuronides is always consistent, and this supports the possible inclusion of CCS values in the annotation procedure.~~

It must however be underlined that data reported in this study are collected for pre-purified samples dissolved in standard solution. Experimental data should be further validated in naturally contaminated urine. However, in consideration ~~of~~with previous studies comparing IM data obtained in solution and in the matrix (Goscinny et al. 2015; Paglia et al. 2015; Regueiro et al. 2016), a good stability of CCS values is expected ~~by~~when changing the matrix.

In our view, the use of IMS is a promising tool for complementing LC-HRMS analysis. In spite of co-elution, differences in MS and MS/MS spectra as well as differences in IM may synergistically support compound identification.

The use of larger sets of compounds for the comparison of eCCS and tCCS may allow ~~to~~ the setting-up and ~~validate~~ validation of mathematical models for the fine tuning of theoretical calculation of CCS values. Prediction of CCS values may be used in a number of applications, among them the generation of libraries to support toxicokinetic studies. ~~without the need of reference materials.~~

However, it must be made clear that IMS data cannot support quantification of compounds without the use of reference compounds. Therefore, in our view, the most promising exploitation of IMS in

the elucidation of urinary biomarkers is the possible generation of a list of prevalent metabolites. This would trigger the interpretation of biological pathways activated by mycotoxin exposure, and would drive the synthesis of prevalent compounds, making them available for quantitative analysis. ~~As well as, it can be used in personalized healthcare interventions for straightforwardly profiling the pattern of biomarkers for multiple mycotoxins exposure.~~

References

Alassane-Kpembi, I., Puel, O., Pinton, P., Cossalter, A.-M., Chou, T.-C. & Oswald, I.P. (2017). Co-exposure to low doses of the food contaminants deoxynivalenol and nivalenol has a synergistic inflammatory effect on intestinal explants. *Archives of Toxicology, 91*, 2677-2687.

Ali, N., Muñoz, K. & Degen, G.H. (2017). Ochratoxin A and its metabolites in urines of German adults—An assessment of variables in biomarker analysis. *Toxicology Letters, 275*, 19-26.

Assunção, R., Silva, M.J. & Alvito, P. (2016). Challenges in risk assessment of multiple mycotoxins in food. *World Mycotoxin Journal, 9* (5), 791-811.

Boschmans, J., Jacobs S., Williams J. P., Palmer M., Richardson K., Giles K., Lapthorn C. L., Herrebout W. A., Lemiere F.& Sobott F. (2016). Combining density functional theory (DFT) and collision cross-section (CCS) calculations to analyze the gas-phase behaviour of small molecules and their protonation site isomers. *Analyst, 141*, 4044-4054.

Campuzano, I., Bush, M.F., Robinson, C.V., Beaumont, C., Richardson, K., Kim, H., Kim, H.I. (2012). Structural characterization of drug-like compounds by ion mobility mass spectrometry:

Formatted: English (United States)

comparison of theoretical and experimentally derived nitrogen collision cross sections. *Analytical Chemistry*, *84*(2), 1026-33.

Cozzini, P. & Dellafiora L. (2012). In silico approach to evaluate molecular interaction between mycotoxins and the estrogen receptors ligand binding domain: a case study on zearalenone and its metabolites. *Toxicology Letters, 214*(1), 81-85.

Cumeras, R., Figueras, E., Davis, C.E., Baumbach, J.I. & Gràcia, I. (2015). Review on ion mobility spectrometry. Part 1: current instrumentation. *Analyst, 140*(5), 1376-1390.

Dall'Asta, C., Berthiller, F., Schuhmacher, R., Adam, G., Lemmens, M. & Krska, R. (2008). DON glycosides: Characterisation of synthesis products and screening for their occurrence in DON treated wheat samples. *Mycotoxin Research, 21*, 123–127.

Dellafiora, L., Galaverna, G. & Dall'Asta, C. (2017). In silico analysis sheds light on the structural basis underlying the ribotoxicity of trichothecenes—A tool for supporting the hazard identification process. *Toxicology Letters, 270*, 80-87.

Dluzen, D.F., Sun, D., Salzberg, A.C., Jones, N., Bushey, R.T., Robertson, G.P. & Lazarus, P. (2014). Regulation of UDP-glucuronosyltransferase 1A1 expression and activity by MicroRNA 491-3ps. *Journal of Pharmacology and Experimental Therapeutics, 348(*3), 465-477.

Dong, D., Ako, R., Hu, M. & Wu, B. (2012). Understanding substrate selectivity of human UDP-glucuronosyltransferases through QSAR modeling and analysis of homologous enzymes. *Xenobiotica, 42*(8), 808-820.

Föllmann, W., Ali, N., Blaszkewicz, M. & Degen, G.H. (2016). Biomonitoring of Mycotoxins in Urine: Pilot Study in Mill Workers. *Journal of Toxicology and Environmental Health - Part A: Current Issues, 79* (22-23), 1015-1025.

Gonzales, G.B., Smagghe, G., Coelus, S., Adriaenssens, D., De Winter, K., Desmet, T., Raes, K. & Van Camp, J. (2016). Collision cross section prediction of deprotonated phenolics in a travelling-wave ion mobility spectrometer using molecular descriptors and chemometrics. *Analytica Chimica Acta*, *924*, 68–76.

Formatted: Font: Italic

Formatted: Font: Italic

Formatted: Italian (Italy)

Goscinny, S., Joly, L., De Pauw, E., Hanot, V. & Eppe, G. (2015). Travelling-wave ion mobility time-of-flight mass spectrometry as an alternative strategy for screening of multi-class pesticides in fruits and vegetables. *Journal of Chromatography A, 1405*, 85-93.

Heyndrickx, E., Sioen, I., Bellemans, M., De Maeyer, M., Callebaut, A., De Henauw, S., De Saeger, S. (2014). Assessment of mycotoxin exposure in the Belgian population using biomarkers: Aim, design and methods of the BIOMYCO study. *Food Additives and Contaminants - Part A Chemistry, Analysis, Control, Exposure and Risk Assessment, 31* (5), 924-931.

Heyndrickx, E., Sioen, I., Huybrechts, B., Callebaut, A., De Henauw, S., De Saeger, S. (2015). Human biomonitoring of multiple mycotoxins in the Belgian population: Results of the BIOMYCO study. *Environment International, 84*, 82-89.

Hove, M., Van Poucke, C., Njumbe-Ediage, E., Nyanga, L.K. &De Saeger, S. (2016). Review on the natural co-occurrence of AFB1 and FB1 in maize and the combined toxicity of AFB1 and FB1. *Food Control, 59*, 675-682.

Kim, S., Thiessen, P.A., Bolton, E.E., Chen, J., Fu, G., Gindulyte, A., Han, L., He, J., He, S., Shoemaker, B.A., Wang, J., Yu, B., Zhang, J. & Bryant, S.H. (2016). PubChem Substance and Compound databases. *Nucleic Acids Research, 44*, 1202-13.

Kim, H., Kim, H.I., Johnson, P.V., Beegle, L.W., Beauchamp J.L., Goddard, W.A., Kanik, I. (2008). Experimental and theoretical investigation into the correlation between mass and ion mobility for choline and other ammonium cations in N 2 . *Analitical Chemistry, 80,* 1928-1936.

Lapthorn C., Pullen F., Chowdhry B., Wright P., Perkins G. & Heredia Y. (2015). How useful is molecular modelling in combination with ion mobility mass spectrometry for 'small molecule' ion mobility collision cross-sections? *Analyst, 140* (20), 6814-6823.

Mason, E.A., Schamp, H.W. (1985). Mobility of gaseous lons in weak electric fields. *Annals of Physics*, *4*(3), 233–270.

Maul, R., Warth, B., Kant, J.S., Schebb, N.H., Krska, R., Koch, M. & Sulyok, M. (2012). Investigation of the Hepatic Glucuronidation Pattern of the Fusarium Mycotoxin Deoxynivalenol in Various Species. *Chemical Research in Toxicology, 25*, 2715−271.

Maul, R., Warth, B., Schebb, N.H., Krska, R., Koch, M., Sulyok, M. (2015). In vitro glucuronidation kinetics of deoxynivalenol by human and animal microsomes and recombinant human UGT enzymes. *Archives of Toxicology, 89* (6), 949-960.

May, J.C., Goodwin, C.R., Lareau, N.M., Leaptrot, K.L., Morris, C.B., Kurulugama, R.T., Mordehai, A., Klein, C., Barry, W., Darland, E., Overney, G., Imatani, K., Stafford, G.C., Fjeldsted, J.C. & McLean, J.A. (2014). Conformational Ordering of Biomolecules in the Gas Phase: Nitrogen Collision Cross Sections Measured on a Prototype High Resolution Drift Tube Ion Mobility-Mass Spectrometer. *Analitycal Chemistry, 86*, 2107−2116.

Mesleh, M. F., Hunter, J. M., Shvartsburg, A. A., Schatz, G. C., Jarrold, M. F. (1996). Structural Information from Ion Mobility Measurements: Effects of the Long Range Potential. *Journal of Physical Chemistry*, *100*, 16082-16086.

~~Mukherjee, D., Royce, S.G., Alexander, J.A., Buckley, B., Isukapalli, S.S., Bandera, E.V., Zarbl, H. & Georgopoulos, P.G. (2014). Physiologically based toxicokinetic modeling of zearalenone and its metabolites: Application to the Jersey girl study. *PLoS ONE, 9* (12), art. no. e113632.~~

Paglia, G., Angel, P., Williams, J.P., Richardson, K., Olivos,H.J., Thompson,J.W., Menikarachchi, L., Lai,S., Walsh, C., Moseley, A., Plumb, R.S., Grant, D.F., Palsson, B.O., Langridge, J., Geromanos, S. & Astarita, G. (2015). Ion Mobility-Derived Collision Cross Section as an Additional Measure for Lipid Fingerprinting and Identification. *Analytical Chem*istry, *87,* 1137-1144.

Paglia, G., Kliman, M., Claude, E., Geromanos, S. & Astarita, G. (2015). Applications of ion-mobility mass spectrometry for lipid analysis. *Analitycal and Bionalytical Chemistry*, *407*, 4995-5007.

527 Pettersen, E.F., Goddard, T.D., Huang, C.C., Couch, G.S., Greenblatt, D.M., Meng, E.C. & Ferrin,
528 T.E. (2004). UCSF Chimera--a visualization system for exploratory research and analysis. *Journal*
529 *of Computational Chemistry, 25*(13), 1605-12.
530
531 Pfeiffer, E., Schmit, C., Burkhardt, B., Altemöller, M., Podlech, J. & Metzler, M. (2009).
532 Glucuronidation of the mycotoxins alternariol and alternariol-9-methyl ether in vitro: Chemical
533 structures of glucuronides and activities of human UDP-glucuronosyltransferase isoforms.
534 *Mycotoxin Research, 25* (1), 3-10.
535
536 Pfeiffer, E., Hildebrand, A., Mikula, H. & Metzler, M. (2010). Glucuronidation of zearalenone,
537 zeranol and four metabolites in vitro: formation of glucuronides by various microsomes and human
538 UDP-glucuronosyltransferase isoforms. *Molecular nutrition and food research, 54* (10), 1468-1476.
539
540 Righetti, L., Paglia, G., Galaverna, G. & Dall'Asta, C. (2016). Recent Advances and Future
541 Challenges in Modified Mycotoxin Analysis: Why HRMS Has Become a Key Instrument in Food
542 Contaminant Research. *Toxins, 8*, 361.
543
544 Ritter, J.K. (2000). Roles of glucuronidation and UDP-glucuronosyltransferases in xenobiotic
545 bioactivation reactions. *Chemico-Biological Interactions, 129* (1-2), 171-193.
546
547 Shirima, C.P., Kimanya, M.E., Routledge M.N., Srey, C, Kinabo, J.L., Humpf, H.U., Wild, C.P.,
548 Tu, Y.K. & Gong, Y.Y. (2015). A prospective study of growth and biomarkers of exposure to
549 aflatoxin and fumonisin during early childhood in Tanzania. *Environmental Health Perspectives,*
550 *123*, 173-178.
551
552 Smith, M.C., Madec, S., Coton, E. & Hymery, N. (2016). Natural Co-occurrence of mycotoxins in
553 foods and feeds and their in vitro combined toxicological effects. *Toxins, 8* (4), art. no. 94.
554
555 Tripathi, S.P., Bhadauriya, A., Patil, A., Sangamwar, A.T. (2013). Substrate selectivity of human
556 intestinal UDP-glucuronosyltransferases (UGTs): In silico and in vitro insight. *Drug Metabolism*
557 *Reviews, 45* (2), 231-252.
558

559 Uhlig, S., Ivanova, L. & Fæste, C.K. (2013). Enzyme-Assisted Synthesis and Structural
560 Characterization of the 3-, 8-, and 15-Glucuronides of Deoxynivalenol. *Journal of Agricultural and*
561 *Food Chemistry*, *61*, 2006–2012.
562
563 Videmann, B., Koraichi, F., Mazallon, M. & Lecoeur, S. (2012). Effect of gender, pregnancy and
564 exposure conditions on metabolism and distribution of zearalenone in rats. *World Mycotoxin*
565 *Journal, 5* (1), 57-69.
566
567 Wallin, S., Gambacorta, L., Kotova, N., Warensjö Lemming, E., Nälsén, C., Solfrizzo, M. & Olsen,
568 M. (2015). Biomonitoring of concurrent mycotoxin exposure among adults in Sweden through
569 urinary multi-biomarker analysis. *Food and Chemical Toxicology, 83*, 133-139.
570
571 Warth, B., Sulyok, M., Fruhmann, P., Berthiller, F., Schuhmacher, R., Hametner, C., Adam, G.,
572 Fröhlich, J. & Krska, R. (2012). Assessment of human deoxynivalenol exposure using an LC–
573 MS/MS based biomarker method. *Toxicology Letters, 211*, 85–90.
574
575 Warth, B., Sulyok, M., Berthiller, F., Schuhmacher, R. & Krska, R. (2013). New insights into the
576 human metabolism of the Fusarium mycotoxins deoxynivalenol and zearalenone. *Toxicology*
577 *Letters, 220* (1), 88-94.
578
579 Warth, B., Sulyok, M. & Krska, R. (2013). LC-MS/MS-based multibiomarker approaches for the
580 assessment of human exposure to mycotoxins. *Analytical and Bioanalytical Chemistry, 405* (17),
581 5687-5695.
582
583 Welsch, T. & Humpf, H.-U. (2012). HT-2 toxin 4-glucuronide as new T-2 toxin metabolite:
584 Enzymatic synthesis, analysis, and species-specific formation of T-2 and HT-2 toxin glucuronides
585 by rat, mouse, pig, and human liver microsomes. *Journal of Agricultural and Food Chemistry, 60*
586 (40), 10170-10178.
587
588 Wu, B., Basu, S., Meng, S., Wang, X. & Hu, M. (2011). Regioselective sulfation and
589 glucuronidation of phenolics: Insights into the structural basis. *Current Drug Metabolism, 12* (9),
590 900-916.
591

Yasar, U., Greenblatt, D.J., Guillemette, C. & Court, M.H. (2013). Evidence for regulation of UDP-glucuronosyltransferase (UGT) 1A1 protein expression and activity via DNA methylation in healthy human livers. *Journal of Pharmacy and Pharmacology, 65* (6), 874-883.

Zachariasova, M., Vaclavikova, M., Lacina, O., Vaclavik, L. & Hajslova, J. (2012). Deoxynivalenol Oligoglycosides: New "Masked" Fusarium Toxins Occurring in Malt, Beer, and Breadstuff. *Journal of Agricultural and Food Chemistry, 60*, 9280-9291.

Acknowledgement

The work was undertaken within the following projects supported by Czech Science Foundation (GACR), No. 16-06008S: A novel comprehensive strategy for assessment of biological effects elicited by mixtures of chemicals occurring foods and food supplements.

This work was also supported by the "Operational Programme Prague – Competitiveness" (CZ.2.16/3.1.00/21537 and CZ.2.16/3.1.00/24503) and the "National Programme of Sustainability I" - NPU I (LO1601 - No.: MSMT-43760/2015).

Formatted: Font: Times New Roman, English (United States)

Formatted: Line spacing: Double

Figure captions

Figure 1. Chemical structures of alternariol (AOH), alternariol monomethyl ether (AME), zearalenone (ZEN), and deoxynivalenol (DON). Possible sites of glucuronidation, are highlighted in gray.

Figure 2 AOH glucuronides UHPLC profile and HRMS/MS spectrum (CE 20 eV).

Figure 3. 3-D structure and CCS values of mycotoxin-glucuronide isomers evaluated in this study. Soft surfaces were added to emphasize the overall shape of the molecule; the blue areas represent the glucuronide linked to the available hydroxyl groups.

Figure 4. Correlation between theoretical (tCCS) and experimental (eCCS) collision cross section values.

Figure(s)

Click here to download high resolution image

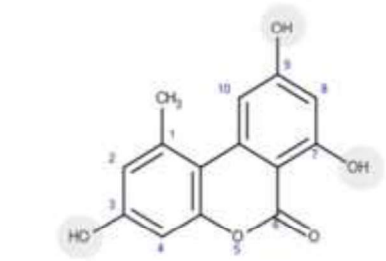

Alternariol
AOH

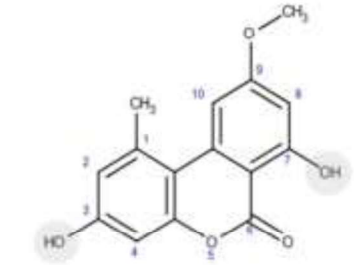

Alternariol mono methyl ether
AME

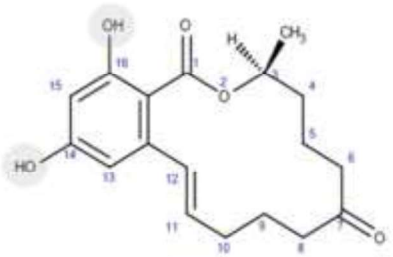

Zearalenone
ZEN

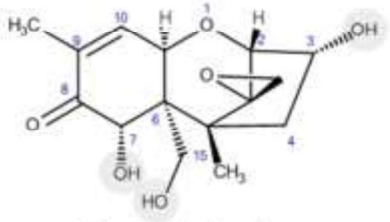

Deoxynivalenol
DON

Figure(s)
Click here to download high resolution image

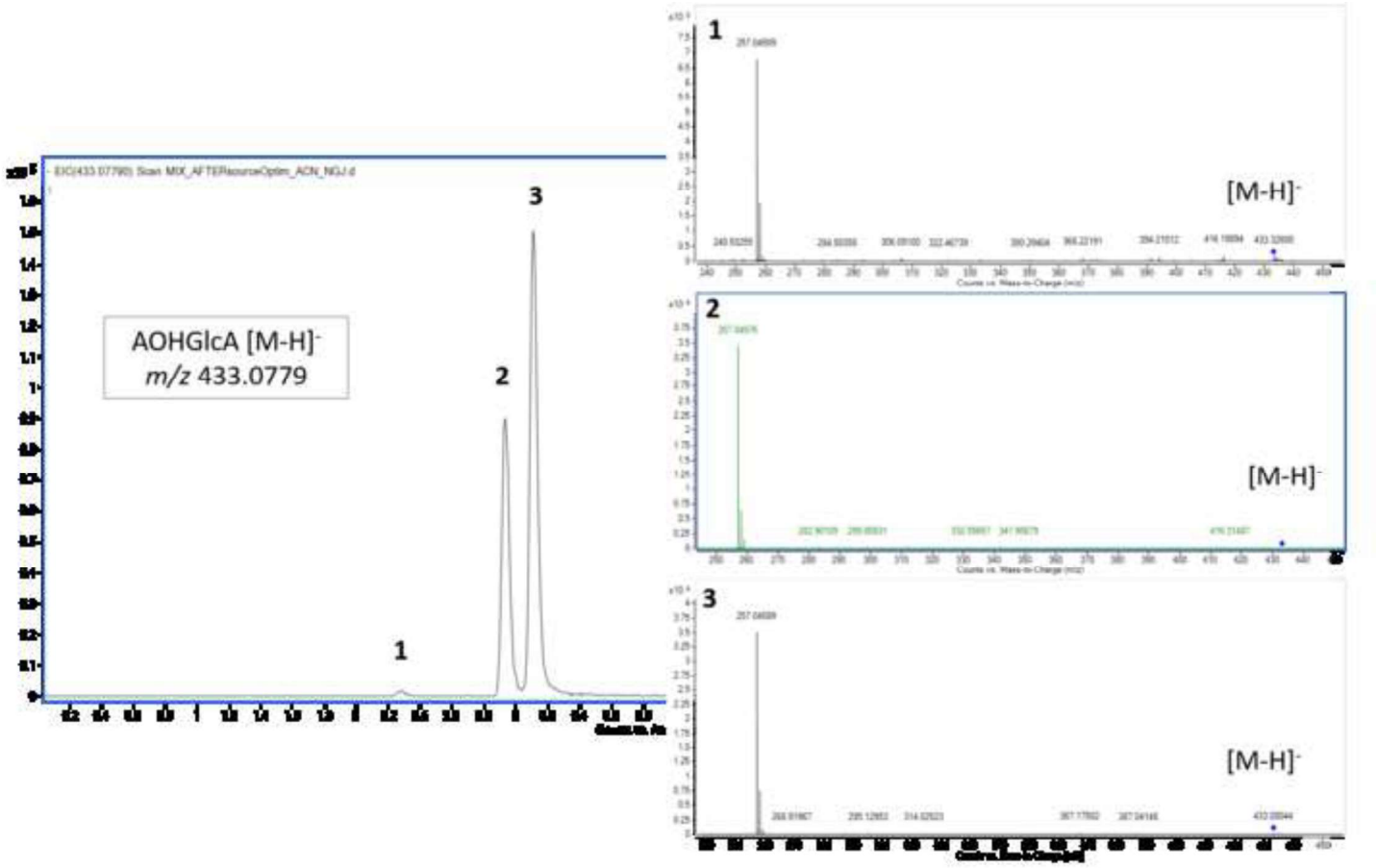

Figure(s)
Click here to download high resolution image

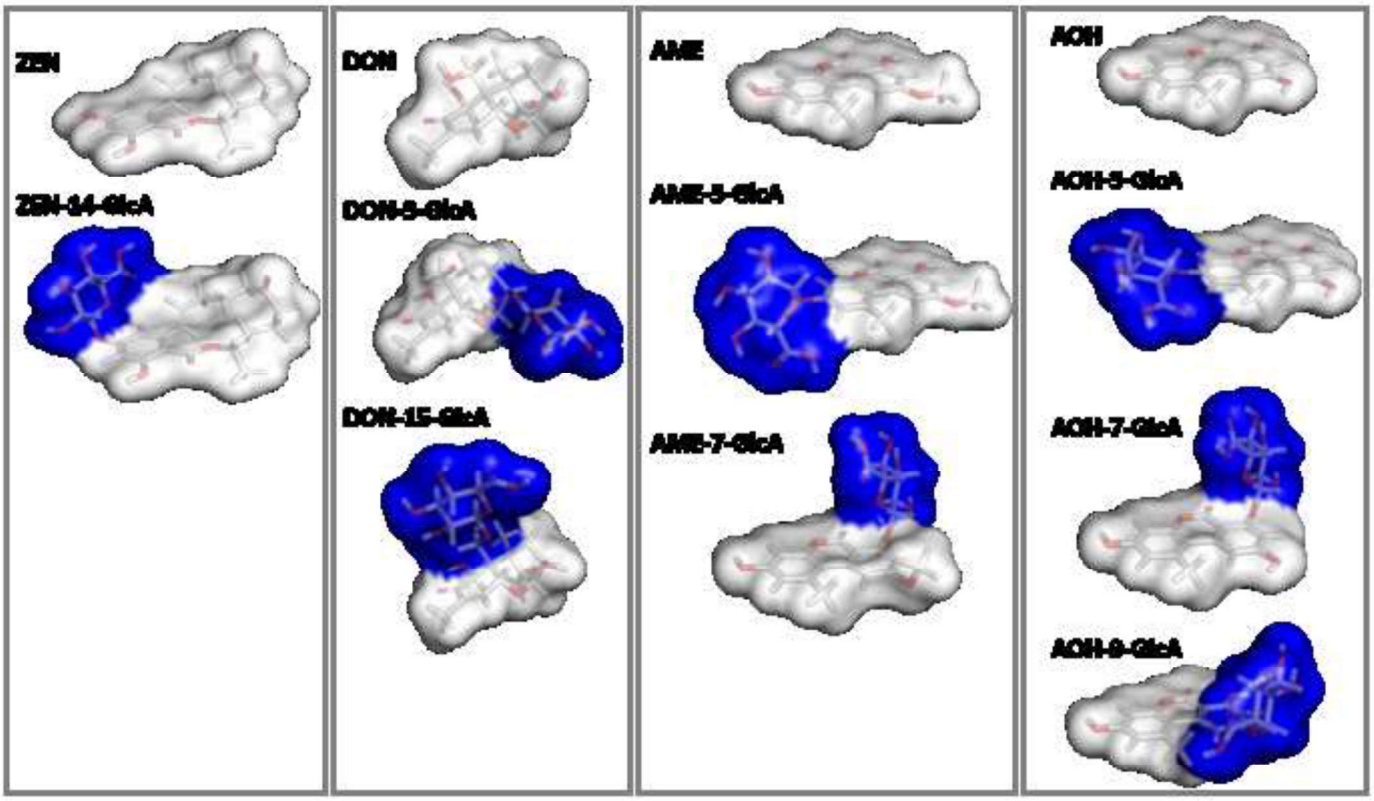

Figure(s)
Click here to download high resolution image

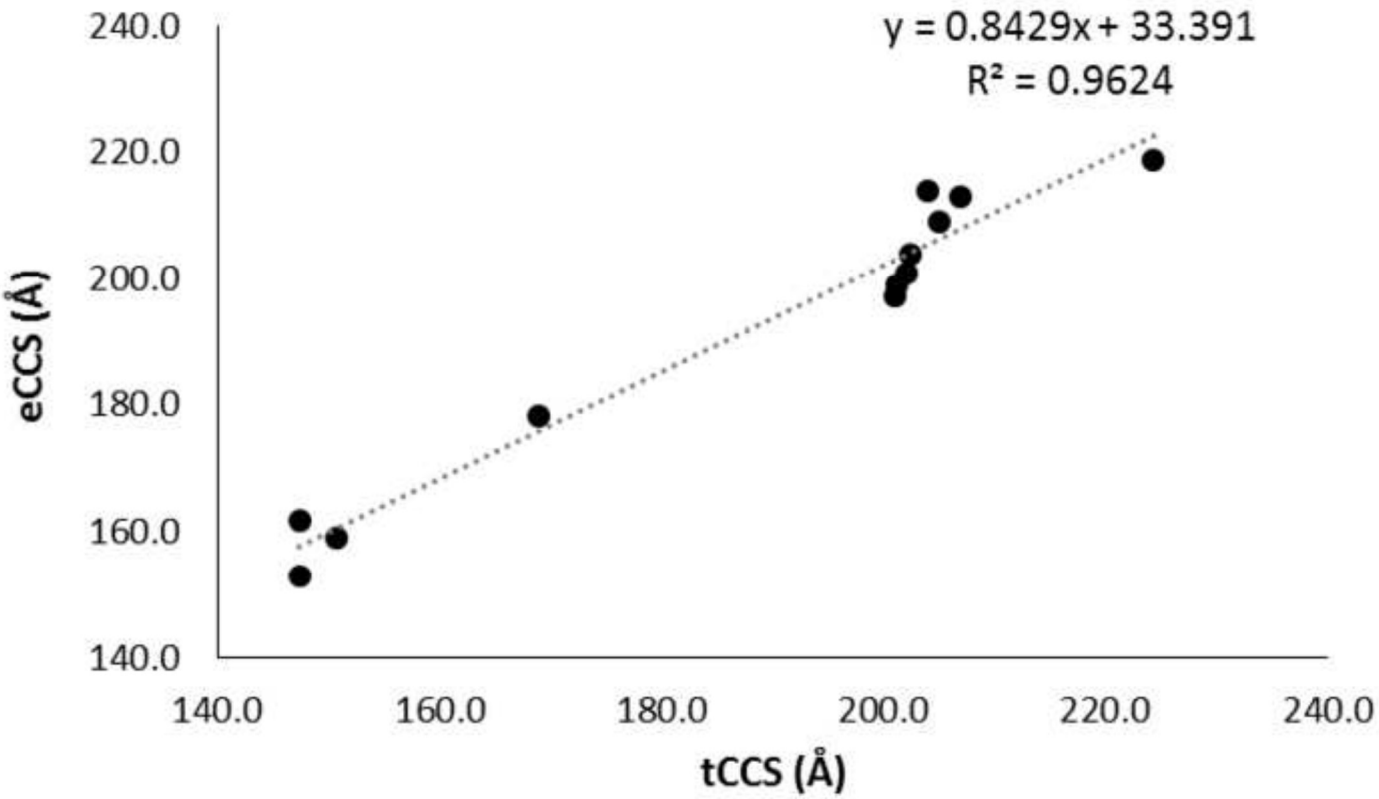

Table(s)

Table 1. HRMS characterization of mycotoxin metabolites obtained after incubation with human liver microsomes.

mycotoxin	elemental composition	detected *m/z* $[M - H]^-$	error (ppm)	MS/MS fragments
ZEN-GlcA	$C_{24}H_{30}O_{11}$	493.172	–1.0	317.1395; 175.0245
DON-3GlcA	$C_{21}H_{28}O_{12}$	471.151	–0.4	441.1422; 265.1109; 217.0890
DON-15GlcA		471.1513	–1.1	265.1092; 217.0890
AME-3GlcA	$C_{21}H_{20}O_{11}$	447.0928	1.1	271.0609; 175.0237
AME-7GlcA		447.0938	–1.1	271.0611; 175.0242
AOH-9GlcA	$C_{20}H_{18}O_{11}$	433.0779	–0.7	257.0456; 175.0239
AOH-3GlcA		433.0775	0.2	257.0459; 175.0241
AOH-7GlcA		433.0785	–2.1	257.0460; 175.0245

Table(s)

Table 2. Summary of drift time and CCS values obtained for each parent and modified mycotoxin. The percentage ~~of~~ error is calculated as the deviation between the experimental CCS and those computationally calculated.

~~M~~mycotoxin	*m/z*	~~V~~volume ($Å^3$)	~~A~~area ($Å^2$)	~~E~~experimental CCS (Å)	~~T~~theoretical CCS (Å)		~~E~~error (%)
				~~CCS (Å)~~	~~A~~av~~are~~erage	SD (%)	
AOH	257.045	197	212	153	147.4	3.4	3.8
AOH-9GlcA	433.0779	333.9	323.1	197.1	202.5	4.6	−2.7
AOH-3GlcA	433.0775	329.9	334.8	203.8	201	4.1	1.4
AOH-7GlcA	433.0785	332.9	330.8	213.8	204.1	4.5	4.8
AME	271.0606	212	227	159	150.7	2.8	5.5
AME-7GlcA	447.0938	355.4	342.5	209	205.1	2.7	1.9
AME-3GlcA	447.0928	345.9	344.6	213	207	3.7	2.9
ZEN	317.1389	280.1	279.2	178.2	169	4.6	5.4
ZEN-14GlcA	493.172	418.9	397.2	218.8	224.4	3.9	−2.5
DON	295	244.5	225.3	161.7	147.4	4.0	9.7
DON-15GlcA	471.1513	383.5	375	199	202.3	3.0	−1.6
DON-3GlcA	471.151	377.3	366	200.7	202.2	3.6	−0.7

Formatted Table

Supplementary Material

Click here to download Supplementary Material: Supplementary material_ok.docx